Published in final edited form as:

FASEB J. 2020 June ; 34(6): 8341–8356. doi:10.1096/fj.201902825RR.

Innate tissue properties drive improved tendon healing in MRL/MpJ and harness cues that enhance behavior of canonical healing cells

Juan Paredes[1], **Jason C. Marvin**[1], **Brenna Vaughn**[1], **Nelly Andarawis-Puri**[2,3]

[1]Nancy E. and Peter C. Meinig School of Biomedical Engineering, Cornell University, Ithaca, NY, USA

[2]Sibley School of Mechanical and Aerospace Engineering, Cornell University, Ithaca, NY, USA

[3]Hospital for Special Surgery, New York, NY, USA

Abstract

Development of tendon therapeutics has been hindered by the lack of informative adult mammalian models of regeneration. Murphy Roth's Large (MRL/MpJ) mice exhibit improved healing following acute tendon injuries, but the driver of this regenerative healing response remains unknown. The tissue-specific attributes of this healing response, despite a shared systemic environment within the mouse, support the hypothesis of a tissue-driven mechanism for scarless healing. Our objective was to investigate the potential of MRL/MpJ tendon extracellular matrix (ECM)-derived coatings to regulate scar-mediated healing. We found that deviations in the composition of key structural proteins within MRL/MpJ vs C57Bl/6 tendons occur synergistically to mediate the improvements in structure and mechanics following a 1-mm midsubstance injury. Improvement in mechanical properties of healing MRL/MpJ vs C57Bl/6 tendons that were isolated from systemic contributions via organ culture, highlighted the innate tendon environment as the driver of scarless healing. Finally, we established that decellularized coatings derived from early-deposited MRL/MpJ tendon provisional extracellular matrix (provisional-ECM), can modulate canonical healing B6 tendon cell behavior by inducing morphological changes and increasing proliferation in vitro. This study supports that the unique compositional cues in MRL/MpJ provisional-ECM have the therapeutic capability to motivate canonically healing cells toward improved behavior; enhancing our ability to develop effective therapeutics.

Keywords

decellularization; extracellular matrix; MRL/MpJ; regeneration; tendon; therapeutics

Correspondence: Nelly Andarawis-Puri, Sibley School of Mechanical and Aerospace Engineering, Cornell University, Ithaca, NY 1485, USA. na424@cornell.edu.

AUTHOR CONTRIBUTIONS

J. Paredes, J. C. Marvin, and N. Andarawis-Puri are responsible for study conception and design; J. Paredes, J. C. Marvin, and B. Vaughn are responsible for acquisition of data; J. Paredes, J. C. Marvin, B. Vaughn, and N. Andarawis-Puri are responsible for analysis and interpretation of data; J. Paredes, J. C. Marvin, and N. Andarawis-Puri are responsible for the revision and approval of the manuscript.

CONFLICT OF INTEREST

The authors declare no conflict of interest.

1 | INTRODUCTION

Tendinopathies are debilitating injuries that account for over 30% of musculoskeletal consultations.[1] Tendons typically heal by scar formation, which is structurally and mechanically inferior to the pre-injured tissue. Despite the prevalence of these injuries, current options to treat the scar-mediated response that drives canonical healing are fundamentally ineffective. Furthermore, efforts to identify new potential therapeutics, to improve functional and structural outcomes, have been hindered by the lack of knowledge regarding the biological cues necessary to promote scarless healing in adult mammals.

Recently the Murphy Roth's Large (MRL/MpJ) mouse has been shown as a potential model for adult mammalian regeneration, due to its improved wound healing capacity in a variety of tissues such as ear,[2] intra-articular fractures,[3] and cornea defects.[4] This regenerative healing phenomenon has been shown to be tissue-specific and does not extend to commonly injured tissues such as the skin.[5] However, we and others have recently shown that MRL/MpJ's improved healing capacity extends to acute patellar tendon injuries, suggesting that this mouse can provide a therapeutic template to improve canonical tendon healing.[6–8] However, identifying the drivers of improved tendon healing in MRL/MpJ so that they can be harnessed into therapeutics remains a major hurdle toward translation.

We have previously shown that healing MRL/MpJ tendons exhibit improvements in matrix structure and cell alignment, and possess a unique growth factor environment as early as 1 week following a 0.75-mm acute patellar tendon biopsy punch injury.[6] These early deviations between MRL/MpJ and canonical healing C57Bl/6 (B6) tendons occur during the proliferative phase of healing, where accumulation of a complex provisional extracellular matrix (provisional-ECM) provides a bioactive structural template for subsequent matrix deposition and overall healing. We have also found an absence of correlation between extent of regeneration of ear and tendon injuries despite a similar systemic response in MRL/MpJ healing, providing further support for a focus on the healing tendon composition and structure as drivers of regeneration. However, the rate of wound healing within the body differs depending on the anatomical location and specific environment of each injured tissue, indicating the need for direct investigation of the intrinsic tendon properties as drivers of the improved healing in the MRL/MpJ in isolation from the systemic environment.

The notion of utilizing the naturally deposited extracellular matrix (ECM) scaffold is supported by recent studies in other tissues, which have been interrogating the isolated ECM to develop tissue therapeutics.[9] For instance, decellularized kidney,[10] skeletal muscle,[11] and heart[12] matrices from non-regenerative mammalian models have been utilized in attempts to reprogram cell behavior in vitro and in vivo with the goal of elucidating mechanisms to reverse tissue damage and encourage regeneration. Consequently, the overarching goal of this study is to identify the potential of MRL/MpJ tendon ECM-derived coatings to regulate canonical healing. Our overarching hypothesis is that therapeutic coatings derived from MRL/MpJ tendon ECM can harness the cues to guide cells from a canonical tendon healing model toward the cellular behavior characteristic of a regenerative healing model under in vitro conditions.

We conducted three experiments to interrogate our overarching hypothesis. First, we set out to confirm that MRL/MpJ's regenerative healing capacity still extends to a larger tendon defect, in comparison to our previous studies, thereby providing a larger region of injury in the tendon midsubstance that could be utilized for therapeutic interrogation. Previous studies have shown that injury size affects the regenerative outcome within the MRL/MpJ. For instance, while 2-mm full-thickness ear cartilage injuries in the MRL/MpJ have been shown to heal through a scarless-mediated mechanism of complete wound closure after 25 days,[13] 4-mm in diameter injuries do not reach full tissue closure and heal through scarring even after 85 days of healing.[14] Furthermore, synergistically to the previously analyzed growth factor environment, we evaluated the large structural components of this provisional-ECM, including collagen I,[15,16] collagen III,[17] decorin,[18] and fibromodulin,[19] in the context of regenerative tendon healing, given their known roles in modulating tendon function, scarring, fibrillogenesis, and growth factor sequestration.[20] Our first hypothesis was that compositional differences in the provisional-ECM of MRL/MpJ will be apparent by the early proliferative stage of healing.

Our second experiment utilized organ culture to determine the ability of the MRL/MpJ innate tendon environment to drive scarless healing in the absence of systemic contributions. As previously stated, we have recently shown that the MRL/MpJ exhibits a similar inflammatory response following ear and tendon injuries.[6] Yet, no correlations have been found between the level of healing of scarless-mediated ear punch injuries and patellar tendon alignment, hyaluronan content, growth factor concentration, or cell behavior.[6] These findings, coupled with the tissue specificity of the scarless healing response, allude that the systemic environment is not the driver of regeneration in the MRL/MpJ, but do not directly isolate the contribution of the systemic from the local tendon environment in healing. We hypothesized that MRL/MpJ tendons will continue to exhibit an improved healing response compared to B6 mice after 4 weeks in organ culture despite isolation from the systemic environment.

Finally, as a step toward utilization of the provisional-ECM for therapeutic potential, in our third experiment, we interrogated the efficacy of early-deposited MRL/MpJ provisional-ECM in modulating canonical healing B6 tendon cell activity in vitro using tissue-specific decellularized ECM-derived coatings. Previous studies have shown that a single application of ECM produced by cells isolated from healing MRL/MpJ ear punches was able to induce regenerative healing of scar-mediated healing B6 dermis in a full-thickness dorsal skin injury.[21] However, no previous studies have been performed to assess the ability of the MRL/MpJ tendon ECM to stimulate a regenerative response on canonical healer B6-derived cells. We hypothesized that the different compositional properties of decellularized MRL/MpJ provisional-ECM compared to B6 provisional-ECM will provide a biological environment that modifies B6 cell behavior, highlighting the potential utility of MRL/MpJ matrix-driven therapeutics to improve tendon healing. Identification of early changes in the in vivo compositional behavior of vital structural matrix components within the MRL/MpJ compared to B6 tendons, coupled with the assessment of the innate tendon environment as the driver of regeneration will further elucidate the effectiveness of the MRL/MpJ ECM in providing the regenerative cues necessary to develop future tendon therapeutics.

2 | MATERIALS AND METHODS

2.1 | Midsubstance patellar tendon punch injury

Under IACUC approval, a full-thickness hole punch injury was introduced into the midsubstance of male MRL/MpJ (n = 65) and B6 (n = 67) left patellar tendons at 16 weeks of age.[6] Briefly, mice were placed under isoflurane (2% by volume, 0.3 L/min), fur was removed from the entire leg, and the patellar tendon was exposed through a skin incision above the patellar tendon. A stainless-steel backing coated with a thin layer of polyurethane was introduced beneath the tendon, and a 1-mm biopsy punch was utilized to create the defect. The backing was then removed, and skin incision was sutured utilizing commercially available 6–0 Prolene sutures (Ethicon Inc, Somerville, NJ, USA). Right tendons were utilized as uninjured controls. Following the procedure, analgesic (Buprenorphine, 0.2 mg/kg) was administered and mice were allowed to resume cage activity until the time of sacrifice. With IACUC approval, MRL/MpJ and B6 mice were obtained directly from The Jackson Laboratory (MRL/MpJ #000486 & B6 #000664, Bar Harbor, ME, USA) (n = 155) and a subset were bred in house (MRL/MpJ n = 5) with the original dame and sire obtained from The Jackson Laboratory (MRL/MpJ #000486, Bar Harbor, ME, USA).

2.2 | Analysis of structure and mechanics of in vivo healing MRL/MpJ and B6 tendons

A subset of patellar tendons were dissected, fixed in zinc buffered formalin, embedded in paraffin, and sectioned (8 μm/section) for microscale structural analysis via fluorescent imaging. Tendon sections were imaged at 10X magnification utilizing a fluorescence microscope under a blue light filter to capture the tissue structural auto-fluorescence. A previously validated custom MATLAB code was used to quantify the fraction of aligned matrix deposited at the injury site for both MRL/MpJ and B6 tendons at 1 (n = 8/strain) and 6 weeks (n = 7–8/strain) post-injury.[6]

Following dissection, injured (n = 8–9/strain) and uninjured control (n = 8/strain) tendons were placed in a 1X PBS bath at room temperature for mechanical testing. An initial 0.2 N preload was applied, and tendons were preconditioned for 15 cycles at 1% strain, with a frequency of 1 Hz. Stress relaxation testing was performed at 5% strain for 300 seconds. Load was then removed, and tendons were allowed to recover for 300 seconds between tests. Preconditioning was reapplied for 15 cycles (1% strain, 1 Hz). Finally, pull to failure testing was performed at a rate of 0.1% strain/second. Ultimate load and stiffness were calculated. Digital images were taken utilizing a monochrome industrial camera (DMK 33UX250) at a 0.2 N nominal load prior to mechanical testing to measure cross sectional area.

2.3 | Analysis of provisional-ECM composition of in vivo healing MRL/MpJ and B6 tendons

Immediately post-sacrifice, the midsubstance region of MRL/MpJ and B6 injured (n = 8/strain/timepoint) and uninjured control (n = 8/strain/timepoint) tendons were dissected and placed individually in 1 mL of Deionized (DI) water supplemented with 1X Halt protease inhibitor cocktail (Thermo Fisher Scientific, Waltham, MA, USA). Samples were then flash frozen in liquid nitrogen and lyophilized for 48 hours to ensure all water content was removed from the tendons. A progression of four homogenization cycles (15 seconds/cycle)

was then performed utilizing 2.8-mm in diameter ceramic beads followed in sequence by 1.4-mm diameter beads for a total of eight cycles. Tendons were placed at −80°C for 2 minutes between cycles to maintain tissue stability. Homogenized tendons were then digested utilizing individual solutions of 6 M Gdn-HCL to solubilize proteoglycans followed by 0.1 mg/mL of pepsin in 0.05 M of acetic acid (Sigma-Aldrich, St. Louis, MO, USA) to solubilize collagen content (Protocol adapted from Chondrex Inc, Redmond, WA, USA). Samples were maintained at 4°C with agitation (350 rpm) for 72 hours during per digestion. Following individual digestions, samples were centrifuged at 10 000 rpm for 5 minutes. Supernatant was collected in a separate vial and prepared for analysis via colorimetric assay. Gdn-HCL supernatant was utilized to analyze proteoglycan content, while pepsin digest supernatant was utilized to measure collagen content. Commercially available 96-well plate enzyme-linked immunosorbent assay (ELISA) Kits were utilized to measure decorin (Abcam, Cambridge, MA, USA), fibromodulin (LifeSpan BioSciences Inc Seattle, WA, USA), collagen I (LifeSpan BioSciences Inc Seattle, WA, USA), and collagen III (LifeSpan BioSciences Inc Seattle, WA, USA) content in both injured and control samples for both MRL/ MpJ and B6 tendons. Proteins and proteoglycans of interest were normalized to respective total protein content measured with a Pierce BCA Protein Assay kit (Thermo Fisher Scientific, Waltham, MA, USA). Duplicate measures were averaged from each sample for both ELISA and BCA analysis. Optical density of this colorimetric assay was determined using a microplate reader.

2.4 | Assessment of healing tendon mechanical properties post ex vivo organ culture

Immediately after sacrifice, naïve left patellar tendon-tibia complexes were dissected from male 16-week-old MRL/MpJ (n = 14 total) and B6 (n = 14 total) mice. A 1-mm patellar punch injury was introduced into a subset (n = 7/strain) of the dissected tendons under sterile conditions. Injured and uninjured tendons were then mounted into a sterile polycarbonate chamber utilizing a stainless-steel clamp to secure the tibia. 7–0 Vicryl braided sutures (Ethicon Inc, Somerville, NJ, USA) were placed under the patella and a static load of 2.5 N was applied onto the tendons. Samples were then placed into culture utilizing low-glucose Dulbecco's Modified Eagle Medium (DMEM; Corning, Corning, NY) supplemented with 10% of fetal bovine serum (FBS; Corning, Corning, NY, USA), 1% of antibiotic/antimycotic solution (Gibco, Grand Island, NY, USA), and 1% of ascorbic acid for 4 weeks at 37°C with 5% CO_2. Media changes were performed every 2–3 days. At the end of the culture period (4 weeks), tendons were removed from the culture chamber, imaged for cross sectional area measurements, and mechanical testing was performed, as described above, to calculate ultimate load, stiffness, ultimate stress and modulus.

2.5 | Development of decellularized tendon ECM-derived coatings and growth factor analysis

Detergent-free decellularization of mouse patellar tendons was adapted from a published protocol[22] for mouse skeletal muscle. Four experimental groups were harvested after 1-week post-injury as described above: 1) B6 control (C57Bl/6 uninjured control ECM, BC); 2) MRL/MpJ control (MRL/MpJ uninjured control ECM, MC); 3) B6 injured/provisional (BP); and 4) MRL/MpJ injured/provisional (MP). Samples were incubated in 50 nM of Latrunculin B (BioVision, Milpitas, CA, USA) in low-glucose DMEM for 2 hours at 37°C

with agitation (450 rpm) to disrupt actin cytoskeletal networks. All further steps were performed with agitation (450 rpm) at room temperature. All solutions contained 1X Halt protease inhibitor cocktail to minimize proteolytic degradation, and DI water washes were performed for 30 minutes between hypertonic incubation steps. Samples were then incubated in 0.6 M of KCl for 2 hours, 1.0 M of KI for 2 hours, and washed in dH2O for 12 hours before repeating KCl and KI incubations to lyse cells. Finally, samples were incubated in 1X PBS containing 1 kU/mL Pierce Universal Nuclease for Cell Lysis (Thermo Fisher Scientific, Waltham, MA) to remove cellular remnants, washed in 1X PBS for 48 hours to remove residual nuclease, and flash frozen in liquid nitrogen before long-term storage at −80°C.

Decellularized naïve and provisional patellar tendons from B6 and MRL/MpJ mice were lyophilized for 72 hours, homogenized as described above, and solubilized at a concentration of 10 mg dry tissue weight/mL in 1 mg/mL of 0.1 M HCl-pepsin (Sigma-Aldrich, St. Louis, MO, USA) at 4°C with agitation (150 rpm) for 72 hours. Solubilized ECM digest was diluted in 0.1 M of AcOH to a final concentration of 3 mg/mL, aliquoted, and stored at −80°C for long-term storage. Coatings were prepared by incubating 40 μL of ECM digest in flat-bottomed 96-well plates (Corning, Corning, NY, USA) at 4°C for 18 hours to facilitate optimal protein adsorption. Rat tail type I collagen (Gibco, Grand Island, NY, USA) was incubated similarly and served as a control for wound closure and cell morphology experiments. All coatings were rinsed twice with 1X PBS immediately prior to use to remove residual acid.

To assess differences in B6 and MRL/MpJ growth factor compositions, decellularized control and provisional-ECM digests (n = 3/group) were analyzed using a RayBiotech C-Series Mouse Growth Factor Antibody Array Kit (RayBiotech, Norcross, GA, USA). Samples were loaded at a concentration of 200 μg/mL total protein per membrane, as quantified using a Pierce BCA Protein Assay kit (Thermo Fisher Scientific, Waltham, MA, USA), in 1X PBS supplemented with 1X Halt protease and phosphatase inhibitor (Thermo Fisher Scientific, Waltham, MA, USA). All incubation steps were performed at room temperature with the maximum times recommended as per the manufacturer’s instructions. Chemiluminescent exposures of BC, MC, BP, and MP were concurrently captured using a ChemiDoc MP imager (Bio-Rad Laboratories, Hercules, CA, USA). Images were analyzed in ImageJ with the background subtracted. All sample spots were normalized to a B6 (for comparisons across strains) or control (for comparisons across within strains) reference membrane using the arithmetic mean of the positive control spots. Semiquantitative measurements of growth factor content were reported as normalized integrated intensity. To determine whether meaningful levels of growth factor content were detected, the normalized integrated intensity had to exceed two standard deviations of the mean of the negative control spots. Fold changes of MRL/MpJ control and provisional-ECM compared to their B6 counterparts were calculated for growth factors detected consistently in at least 2 of 3 technical replicates. Growth factors with at least a two-fold change in content were reported and subsequently grouped together as anti-inflammatory, mitogenic, pro-inflammatory, or angiogenic based on previous reports in the literature.

2.6 | In vitro analysis of cell behavior following decellularized ECM-derived coating stimulation

For isolation and culture of B6 primary patellar tendon cells, tendons from five 16-week-old male B6 mice were dissected, stripped of the tendon sheath and fat pad, pooled, and digested with 2 mg/mL of collagenase type I (Gibco, Grand Island, NY, USA) and 1 mg/mL of collagenase type IV (Gibco, Grand Island, NY, USA) in low-glucose DMEM for 2 hours at 37°C on a rocking shaker. Single-cell suspensions were passed through a 70-μm cell strainer and expanded in low-glucose DMEM supplemented with 10% of lot-selected FBS, 1% of antibiotic/antimycotic, sodium pyruvate, and L-glutamine at 37°C with 5% CO_2. All in vitro experiments were performed at passage three with at least three biological replicates from independent cell batches.

For analysis of cell morphology B6 patellar tendon cells were seeded at 2000 cells/well (n = 9/group) in clear, flat-bottomed 96-well plates in low-glucose DMEM supplemented with 10% of lot-selected FBS, 1% of antibiotics/antimycotic, sodium pyruvate, and L-glutamine. After incubating cells for 18 hours to facilitate cell spreading, cells were fixed with 4% of paraformaldehyde (PFA; Electron Microscopy Sciences, Hatfield, PA, USA) for 20 min. To assess the effect of different decellularized ECM-derived coatings on cell morphology, fixed cells were permeabilized with 0.1% of Triton X-100 (Thermo Fisher Scientific, Waltham, MA, USA) for 15 min, blocked in 2.5% of normal horse serum (Vector Laboratories, Burlingame, CA, USA) for 30 min, and stained with rhodamine-phalloidin (Molecular Probes, Inc, Eugene, OR, USA) and DAPI for 1 hour while covered from light. All incubation steps were performed at room temperature. Fluorescent images of phalloidin-stained samples were taken at 10X using a Zeiss Axio Observer Z1 inverted epifluorescence microscope. Blinded measurements of cell circularity (defined as $4*\pi*\text{area/perimeter}^2$), perimeter, area, and aspect ratio (defined as major_axis/minor_axis) were conducted in ImageJ on a single-cell basis (8 cells/well; n = 72/group).

For cell proliferation, B6 patellar tendon cells were seeded at 10 000 cells/well (n = 6/group) in clear, flat-bottomed 96-well plates in low-glucose DMEM supplemented with 10% of lot-selected FBS, 1% of antibiotics/antimycotic, sodium pyruvate, and L-glutamine. After incubating cells for 4 hours to facilitate complete attachment, cells were washed once with 1X PBS and subsequently cultured in serum-starved (1% lot-selected FBS) DMEM for 3 and 7 days with media changes every 2 days. B6 patellar tendon cells were exposed to serum-starved conditions to suppress proliferation allowing us to isolate the effect of the ECM-derived coatings on cell proliferation while maintaining cell viability and minimizing high serum protein concentrations as a confounding factor. To measure cell proliferation as determined by mitochondrial activity, the MTS assay was performed at each timepoint following a 2 hours reagent incubation period as per the manufacturer's instructions. Relative proliferation (%) compared to non-coated wells (ie, B6 patellar tendon cells cultured in serum-starved media conditions without ECM) was normalized to the average protein adsorbed after coating (n = 6/group) quantified using a Micro BCA kit (Thermo Fisher Scientific, Waltham, MA, USA) as per the manufacturer's instructions.

Furthermore, B6 patellar tendon cells were labeled with CellTracker Green CMFDA Dye (Invitrogen, Carlsbad, CA, USA) and seeded on Oris flat-bottomed 96-well plates (Platypus

Technologies, Madison, WI, USA) at a density of 30 000 cells/well (n = 3/group) in serum-starved DMEM. After incubating cells for 18 hours to facilitate complete attachment and cell cycle synchronization, a 1-mm circular defect was created in each well by removing pre-inserted silicone stoppers. Cells were washed once with 1X PBS to remove debris and subsequently cultured in serum-free DMEM for 24 hours to suppress cell proliferation. Fluorescent images were taken on a Spectra Max i3x Multi-Mode Microplate Reader (Molecular Devices, San Jose, CA, USA) at 0, 12, and 24 hours to monitor cell migration into the defect region. Wound closure activity was analyzed using ImageJ to quantify pre- and post-migration integrated intensity. For analysis of cell proliferation and migration three technical replicates were averaged for each independent cell batch.

2.7 | Statistical analysis

Quantitative data are represented as mean ± standard deviation. A one-way ANOVA with Bonferroni post hoc multiple comparisons test was used to analyze selected comparisons for matrix alignment, and all mechanical testing data. A one-way ANOVA with Sidak post hoc multiple comparisons test was utilized for analysis of selected comparisons for provisional-ECM composition of in vivo healing MRL/MpJ and B6 tendons. For collagen I/III ratio, individual Student t-tests were performed at each timepoint to assess differences across strains. For all compositional assessment, statistical analysis was performed on raw data prior to normalization to respective controls. For cell morphology experiments, a one-way Welch ANOVA with post hoc Games-Howell was performed for selected comparisons. For cell proliferation experiments, a one-way ANOVA with post hoc Bonferroni was performed for selected comparisons. Selected comparisons of relative cell proliferation normalized to total protein adsorbed were performed using nonparametric Mann-Whitney tests corrected by the number of comparisons. For cell migration experiments, a Kruskal-Wallis one-way ANOVA with post hoc Dunn for nonparametric data was performed for selected comparisons (#$P \leq .1$, *$P \leq .05$, **$P \leq .01$, ***$P \leq .001$, ****$P \leq .0001$).

3 | RESULTS

All animals in this study tolerated surgery well and survived until the designated timepoint.

3.1 | Analysis of structure and mechanics of in vivo healing MRL/MpJ and B6 tendons

Results showed significant early improvements in matrix alignment in the MRL/MpJ tendons by 1 week post-injury ($P = .012$) compared to B6. Additionally, similar significant improvements in matrix alignment were identified in the MRL/MpJ tendons by 6 weeks compared to B6 ($P = .0002$) (Figure 1).

By 6 weeks after injury, healing MRL/MpJ tendons exhibited decreased stiffness ($P = .0005$), yet a recovery in ultimate load from uninjured controls (Figure 2A,B). At this timepoint, healing B6 tendons exhibited significant decreases in both stiffness ($P \leq 0.0001$) and ultimate load ($P = .0024$) compared to uninjured controls (Figure 2 A,B). Healing MRL/MpJ tendons showed improvements in stiffness ($P = .0032$) and ultimate load ($P = .0785$) when compared to healing B6 tendons (Figure 2A,B). Assessment of stress

relaxation did not show differences between MRL/ MpJ and B6 healing or control patellar tendons after 6 weeks post-injury (Figure 2E).

Furthermore, analysis of material properties showed improved Young's Modulus and ultimate stress in the injured MRL/MpJ compared to B6 tendons ($P = .0658$, $P = .0919$) at 6 weeks post-injury (Figure 2C,D). The Young's Modulus was significantly lower for both MRL/MpJ and B6 injured tendons compared to respective controls ($P = .0444$, $P = .0005$) (Figure 2C). Injured B6 tendons showed significant decreases and ultimate stress ($P = .0134$) compared to uninjured controls, yet no differences were found in the ultimate stress between injured and uninjured MRL/MpJ tendons (Figure 2D). All samples included in this study failed via rupture at the midsubstance of the tendon during mechanical testing.

3.2 | Analysis of provisional-ECM composition of in vivo healing MRL/MpJ and B6 tendons

At 1 week post-injury, MRL/MpJ healing tendons exhibited significantly higher collagen III content ($P = .0178$) but no difference in collagen I content in comparison to healing B6 tendons. Furthermore, both MRL/MpJ and B6 tendons showed significant increases in collagen III ($P \leq 0.0001$, $P \leq 0.0001$) and decreases in collagen I ($P \leq 0.0001$, $P \leq 0.0001$) content compared to uninjured controls by 1 week post-injury (Figure 3A,B). Additionally, healing MRL/MpJ tendons exhibited significantly higher decorin content ($P = .0117$) in comparison to healing B6 tendons at 1 week post-injury; yet, no differences were found in fibromodulin between mouse strains at this timepoint. Compared to uninjured controls, healing MRL/MpJ tendons presented significantly higher levels of decorin ($P = .0305$), while healing B6 tendons showed lower fibromodulin content ($P = .0573$) at 1 week post-injury (Figure 3C,D).

Examination of the late tendon healing response during remodeling showed significantly lower collagen III content ($P = .0028$) and no difference in collagen I content in the MRL/MpJ tendons compared to B6 after 6 weeks of healing. As expected, healing MRL/MpJ and B6 tendons showed significantly higher collagen III content ($P \leq 0.0001$, $P \leq 0.0001$) compared to uninjured controls by 6 weeks. At this timepoint, collagen I was significantly lower in the healing MRL/MpJ ($P = .0063$) but not B6 tendons in comparison to uninjured controls (Figure 3A,B). Small leucine-rich proteoglycan (SLRP) analysis at the 6 week timepoint showed that healing MRL/MpJ tendons exhibited higher levels of decorin ($P = .1029$) compared to healing B6 tendons. Healing B6 tendons showed a significant decrease in decorin content compared to uninjured controls by 6 weeks post-injury ($P = .0184$). No differences were found in fibromodulin content of healing tendons between strains or relative to uninjured controls at 6 weeks (Figure 3C,D). No differences were found in the collagen I/III ratio between MRL/MpJ and B6 tendons at either 1 or 6W (Figure 3E).

3.3 | Assessment of healing tendon mechanical properties post ex vivo organ culture

There was no difference in stiffness or ultimate load between uninjured MRL/MpJ and B6 tendons after 4 weeks in organ culture (Figure 4A,B). Healing MRL/MpJ tendons showed higher stiffness ($P = .0360$) and ultimate load ($P = .0147$) compared to B6 after 4 weeks in culture, while stiffness and ultimate load were decreased in healing B6 ($P = .0001$, $<.0001$)

and ultimate load was decreased in healing MRL/MpJ tendons ($P = .0209$) compared to uninjured controls (Figure 4A,B).

Additionally, both the Young's Modulus and ultimate stress were higher in injured MRL/MpJ compared to B6 tendons ($P = .0992$, $P = .0972$) after 4 weeks in culture (Figure 4C,D). No differences were identified in the Young's Modulus between injured and uninjured MRL/MpJ tendons after 4 weeks in culture. However, a decrease in ultimate stress was found in the injured MRL/MpJ tendons compared to respective uninjured controls ($P = .116$). Decreases in both Young's Modulus ($P = .0019$) and ultimate stress ($P = .0002$) were found in injured B6 tendons compared to uninjured controls by this timepoint (Figure 4C,D).

3.4 | Growth factor analysis of decellularized ECM

Innate decellularized compositional differences were found (five differentially regulated growth factors), with mitogenic growth factors (FGF-7) and pro-inflammatory (amphiregulin, granulocyte-macrophage colony-stimulating factor (GM-CSF), interleukin-2 (IL-2), and interleukin-7 (IL-7)) cytokines elevated/detected only in MC compared to BC (Figure 5A). A greater number of differentially regulated growth factors (eight total) was found between BP and MP. Mitotic growth factors (IGF-2) and pro-inflammatory cytokines (GM-CSF, granulocyte colony-stimulating factor (GCSF), IL-2, and IL-7) were elevated/detected only in MP compared to BP, but MP exhibited reduced anti-inflammatory (hepatocyte growth factor, HGF) cytokines and angiogenic growth factors (platelet-derived growth factor AA (PDGF-AA) and placental growth factor (PLGF)) (Figure 5B).

3.5 | In vitro analysis of cell behavior following decellularized ECM-derived coating stimulation

Cells cultured on MP exhibited significantly decreased circularity ($P < .0001$) and increased area ($P = .0694$) compared to cells cultured on BP or collagen I, respectively (Figure 6 A,B). Similarly, cells cultured on MC exhibited significantly decreased circularity compared to cells cultured on BC ($P = .003$). No significant differences in circularity were found between strains, but cells cultured on BP exhibited increased area compared to ones cultured on BC ($P = .1256$) and collagen I ($P = .0857$). Cells cultured on BC and BP showed comparable circularity to that of cells in collagen I. (Figure 6A).

Cells cultured on MP showed significantly enhanced cell proliferation compared to BP ($P = .0015$) after 3 days of culture (Figure 7A). No significant differences in cell proliferation were found for all comparisons after 7 days of culture (Figure 7B). After 3 days of culture, relative proliferation normalized to total protein content on a per microgram basis similarly showed that MP significantly enhanced cell proliferation compared to BP ($P = .0058$), suggesting that cell proliferation was driven by compositional differences rather than protein content (Figure 7C). No differences in cell migration were found for all comparisons at each measured timepoint (Figure 8).

4 | DISCUSSION

Development of effective tendon therapeutics to overcome aberrant matrix deposition during canonical healing has been hindered by the lack of informative regenerative healing models. In this study, we have identified that the early-deposited MRL/MpJ provisional-ECM following acute tendon injuries harnesses unique compositional cues that drive the improved tendon healing outcome of this mouse strain and have the therapeutic capability to motivate canonical healing cells toward improved morphological and proliferative behavior.

The wound healing response is complex and can gather cues from both the systemic and innate tissue environment; however, the scarless healing response in the MRL/MpJ has been shown to be tissue-specific suggesting the need to further interrogate the role of the intrinsic tissue properties in its regenerative healing response[2,3,5]. We have previously demonstrated that structural and cellular improvements can be identified in the MRL/ MpJ following a patellar punch injury compared to a canonical healing B6 model, which, similarly to the human tendon healing response, have been shown to heal through deposition of disorganized matrix ultimately leading to scar formation and poor mechanical outcomes.[6,7,18,23] Additionally, regenerative attributes have also been identified following ear punch injuries in the MRL/MpJ[2]; however, despite results showing a similar systemic environment compared to tendon, no correlations were identified between the systemic inflammation and the extent of ear and tendon healing.[6] Together, these findings led us to the overarching hypothesis that therapeutic coatings derived from MRL/MpJ tendon ECM have the potential to provide the necessary cues to guide tendon cell behavior toward improved healing.

An initial step toward interrogating the healing potential of the MRL/MpJ ECM was the assessment of the innate tendon environment as the driver of scarless healing. Thereby, principles of organ culture were utilized to preserve the cell-matrix tendon environment, while removing systemic contributions throughout healing. A key characteristic of uninjured tendons is their ability to resist high levels of tensile loading experienced throughout daily activity; therefore, while histological analysis of the deposited matrix in organ culture was not conducted, mechanical testing provided a robust and stringent assessment of the tendon healing in isolation from the systemic environment. Accordingly, analysis of mechanical improvements accurately identifies the extent of functional recovery following tendon injuries. Results showed no differences in mechanics between uninjured controls after culture, elucidating similar effects of organ culture on patellar tendons regardless of genetic strain. Supporting our hypothesis, analysis of healing tendons showed that MRL/MpJ tendons exhibited improvements in stiffness and ultimate load compared to B6 when separated from the systemic environment. Thereby, elucidating that tissue-specific changes mediated by a unique provisional-ECM in MRL/MpJ tendons serve as the driver of scarless healing.

Further in support of these findings, in vivo assessment of the concentration of key structural matrix components in MRL/MpJ patellar tendon highlighted the promising role of the early-deposited ECM on subsequent healing. Introduction of the biopsy punch injury removes the collagen I rich matrix at the tendon midsubstance, resulting in the decreased levels in collagen I observed in MRL/MpJ and B6 tendons compared to uninjured controls, creating a

defect in which a bioactive provisional-ECM is deposited throughout healing.[20] Interestingly, the early increases in collagen III at the injury site in the MRL/ MpJ compared to B6 tendons could implicate a beneficial role for this structural protein in providing a mechanosensitive cellular template for subsequent matrix deposition. However, the later decrease in collagen III compared to B6 tendons, combined with the increased matrix alignment in the MRL/MpJ, high-lights the need for this collagenous component to be replaced by an organized matrix structure to achieve scarless healing. Assessment of the in vivo healing response in MRL/MpJ and B6 tendons following our modified midsubstance punch injury model showed the expected improvements in stiffness, ultimate load, Young's modulus, and ultimate stress, in healing MRL/ MpJ tendons compared to B6; however, compositional analysis showed that the collagen I/III ratio did not differ between MRL/MpJ and B6 tendons at 6W, and while collagen I returns to uninjured levels in B6 tendons after 6 weeks post-injury, it remained lower in the MRL/MpJ tendons at this timepoint. Collagen I is a key player in allowing healthy tendons to resist the large levels of load applied during locomotion.[24] Therefore, the lack of collagen I recovery in the MRL/MpJ tendons and lack of improvement in the collagen I/III ratio compared to B6 during the late timepoint, despite an improvement in alignment and mechanical properties, was unexpected. Nevertheless, studies have shown that in addition to collagen I content, structural matrix cross-link quality is a key primary regulator of mechanical function.[16,25] For instance, alterations in cross-linking behavior due to increased advanced glycation end products have been shown to modulate failure behavior of tendon fibrils,[26] while others have attributed hydroxylysyl-pyridinoline cross-link density, mediated by lysyl-oxidase, to the resulting stiffness changes in tendons throughout aging.[27] Furthermore, secondary regulators, such as collagen fiber diameter, could further explain the unexpected discrepancy between collagen I content and mechanical behavior in the MRL/MpJ tendons.[16,28] Larger, densely packed fibers at the subcellular scale could result in a higher cross-sectional area over which the mechanical loads are distributed, thereby allowing the fibers to withstand higher loads before reaching failure. Additionally, tissue engineering studies have shown that fiber diameter regulates fibroblast growth and differentiation,[29] suggesting a role in modulating the structural matrix quality deposited by these cells. Potential improvements in fiber and cross-linking quality coupled with our observed improvement in fiber alignment in healing MRL/MpJ tendons could help explain the resulting mechanical improvements post-injury despite the decrease in collagen I and lack of improvements in the collagen I/III ratio; however, further assessment of fiber structure and cross-linking profile of healing MRL/MpJ and B6 tendons is necessary to confirm this notion.

Additionally, we have previously shown that Transforming Growth Factor-β (TGF-β), a soluble growth factor implicated in fibrosis, is significantly decreased in the MRL/MpJ compared to B6 after patellar tendon injury in vivo.[6] Interestingly, in this study, we found higher levels of decorin, a SLRP demonstrated to play a major role in the sequestration of this growth factor,[30] in the early-deposited ECM of MRL/MpJ tendons compared to B6. The presence of decorin has been shown to inhibit the TGF-β signaling pathway,[31] which coupled with the previously observed decreases in this cytokine's concentration in the MRL/MpJ tendons after injury, could provide a possible mechanism responsible for the scarless healing observed in this model. On the other hand, the collagen-binding SLRP

fibromodulin provides a functionally active ECM for tendon stem-like progenitor cells by modulating their interactions with growth factors associated with aberrant matrix deposition such as TGF-β and Bone Morphogenetic Proteins (BMPs).[32,33] Unexpectedly, no differences were identified in fibromodulin content between MRL/MpJ and B6 tendons throughout injury. However, we found an early decrease in the presence of fibromodulin in healing B6 tendons when compared to uninjured controls. Studies have shown that while fibromodulin is fundamental for regeneration of cutaneous wound healing observed during fetal stages,[34] decreased levels of this SLRP result in hypertrophic scar formation in adult models.[35,36] Therefore, it is possible that, early maintenance of fibromodulin levels observed in MRL/MpJ tendons compared to controls, in contrast to the decrease observed in healing B6 tendons, are sufficient for successful contribution of this SLRP toward a synergistic ECM environment that leads to regeneration. Collectively, this data suggest that tissue-specific changes mediated by a unique provisional-ECM in MRL/MpJ tendons serve as the driver of scarless healing.

The intrinsic tendon environment is composed of both resident cells and matrix that are responsible for the ensuing healing response in vivo.[16] However, introduction of cellular components from one host to another has been shown to have potential adverse effects such as high risks for infection and rejection of the transplanted therapeutics or grafts.[37] To overcome this limitation, decellularized constructs that maintain ECM environmental cues without cell debris have become viable products for therapeutic applications.[38–40] Interestingly, a number of studies have shown the ability of decellularized matrices to stimulate improved healing and cell behavior in tissues such as the heart,[41] skeletal muscle, [42] brain,[43] and adipose.[44] Still, whether the in vivo early compositional and growth factor environment in MRL/MpJ could be harnessed toward effective tendon therapeutic strategies remained unknown. Therefore, we interrogated the capacity of the early-deposited MRL/MpJ provisional-ECM composition to modulate B6 tendon-derived cell activity in vitro. To isolate the therapeutic effect of different MRL/MpJ and B6 ECM compositions on B6 derived cells, we utilized a non-proteolytic detergent-free decellularization protocol that eliminated cell-associated influences while preserving the natural composition and growth factor environment within our coatings. Single-cell analysis of cytoskeletal networks from MRL/MpJ ECM treated cells revealed a dendritic-like phenotype, marked by increased presence of cellular protrusions and decreased circularity (ie, increased cell spreading), compared to cells cultured on B6 ECM. Previous studies have implicated a role for tenocyte protrusions and spreading in mechano-transduction processes vital for ECM production[45] and intercellular communication via formation of gap junctions.[46,47] Furthermore, decreased cell circularity has been associated with actively proliferating cells in low-density 2D cultures,[48] suggesting that the compositional components of MRL/MpJ provisional-ECM provide biochemical cues that facilitate enhanced cell morphological and mitogenic behavior.

Interestingly, early increases in cell proliferation have also been identified as a hallmark of tendon regeneration in the MRL/MpJ.[8] In accordance with these studies, our data showed that MRL/MpJ provisional-ECM enhanced the proliferation of B6 cells compared to B6 provisional-ECM in vitro, further suggesting the promising ability of MRL/MpJ ECM-derived therapeutics to stimulate improved cell behavior of canonically healing tendon

injuries. Notably, elevated levels of pro-inflammatory factors GM-CSF, GCSF, IL-2, and IL-7, implicated in the activation of resident tendon cells for effective healing,[49] and mitogenic IGF-2, shown to stimulate tendon cell proliferation,[50,51] were found in MRL/MpJ provisional-ECM indicating that MRL/MpJ tendons harness distinct biological cues during healing. The effect of these ECM-derived coatings on canonically healing tendon cells illustrate that synergistic compositional differences in both uninjured and provisional MRL/MpJ ECM, compared to their B6 counterparts, play a crucial role in mediating effective cellular processes required for scarless tendon healing.

This study is not without some limitations. Tendon area was calculated through visual interpretation from digital images obtained under a nominal load prior to mechanical testing. As a small soft connective tissue, the mouse patellar tendon does not have exact boundaries or edges that can be consistently identified in images; thereby, slight misalignment or rotation of the tissue during imaging could lead to a significant misrepresentation of the tendon's cross sectional area, limiting the accuracy of material property measurements such as Young's modulus and ultimate stress. Adoption of precise laser-based methods[52] or ultrasound imaging[53] could be utilized in future studies to increase the accuracy of cross sectional area measurements. Analysis of the decellularized ECM growth factor environment was limited to semiquantitative evaluation. Thus, future studies employing quantitative measurements of growth factor content and activity are merited to further interrogate the role of these ECM-associated soluble factors in promoting scarless tendon healing. To minimize the confounding effect of serum proteins on cell proliferation, the effect of ECM-derived coatings on cell proliferation was determined under serum-starved conditions up to 7 days. Consequently, a limitation of this approach is that cellular stress due to prolonged serum starvation could also have contributed to changes in cell mitochondrial activity. Future work could measure active DNA synthesis (eg, 5-ethynyl-2′-deoxyuridine or EdU staining) and cell cycle kinetics in vitro to further investigate the influence of our decellularized ECM-derived coatings on cell proliferation. In addition, while the decellularized ECM-derived coatings employed in this study assessed the effect of structural ECM components on cell behavior, this 2D culture model does not fully recapitulate the spatial organization or biochemical properties of the native ECM. Future work should examine cell-ECM interactions and morphological behavior within 3D ECM-derived hydrogels. Furthermore, no changes in cell migration were found in our study, suggesting that early alterations in cell migration may not be a critical contributor to MRL/MpJ scarless tendon healing. However, a 3D ECM environment with chemotactic stimuli (eg, paracrine factors) may be needed to definitively ascertain the role of cell migration during MRL/MpJ scarless tendon healing. Moreover, while we have identified improvements in the healing response of MRL/MpJ by 6W in vivo and therapeutic potential for MRL/ MpJ ECM-derived coatings by 3 days in vitro, future analysis of later timepoints are necessary to ensure persistence of these outcomes. Finally, a limitation of this study is that only male mice were analyzed. Differences in the MRL/MpJ healing response due to sex have been identified in tissues such as ear and articular cartilage.[3,54,55] Accordingly, future work should determine the extent to which our findings extend to the healing response of female MRL/MpJ mice.

Overall, we have shown that the ability of the MRL/MpJ patellar tendons to heal through a scarless-mediated pathway is driven by an intrinsic ECM environment. Furthermore, the

distinctive decellularized composition of MRL/MpJ patellar tendons is able to enhance canonical healing B6 cell activity in vitro. These findings support the therapeutic potential of MRL/MpJ ECM-derived constructs in improving canonical tendon healing. Furthermore, future work elucidating the complete compositional profile and fiber properties, such as diameter and density, of these MRL/MpJ ECM-derived constructs could provide insight into the development of tissue-engineering scaffolds that encourage improved matrix deposition at the injury site. Finally, while in vitro analysis of cell behavior is a necessary first step to identify the therapeutic potential of these MRL/MpJ derived therapeutics, subsequent studies introducing the MRL/MpJ provisional-ECM environment in vivo will provide further insight into the ability of these constructs to promote scarless healing in adult mammals.

ACKNOWLEDGMENTS

The authors acknowledge technical contributions from Dr Claudia Fischbach-Teschl (Cornell University) and Dr Benjamin Cosgrove (Cornell University) for access to their epifluorescence microscope and ChemiDoc MP imager, respectively. This work was supported by the US National Institutes of Health (NIH) Grants NIAMS R01-AR068301 and R01-AR052743 and NSF GRFP DGE-1650441.

Abbreviations:

BC	C57Bl/6 uninjured control ECM
BP	C57Bl/6 provisional-ECM (1-week post-injury)
DI	deionized
ECM	extracellular matrix
ELISA	enzyme-linked immunosorbent assay
FGF-7	fibroblast growth factor 7
GCSF	granulocyte colony-stimulating factor
GM-CSF	granulocyte-macrophage colony-stimulating factor
HGF	hepatocyte growth factor
IGF-2	insulin growth factor 2
IL-2	interleukin-2
IL-7	interleukin-7
MC	MRL/MpJ uninjured control ECM
MP	MRL/MpJ provisional-ECM (1-week post-injury)
MRL/MpJ	Murphy Roth’s Large
PDGF-AA	platelet-derived growth factor AA
PLGF	placental growth factor

Provisional-ECM	provisional extracellular matrix
SLRP	small leucine-rich proteoglycan

REFERENCES

1. Andarawis-Puri N, Flatow EL. Promoting effective tendon healing and remodeling. J Orthop Res. 2018;36(12):3115–3124. [PubMed: 30175859]
2. Heber-Katz E The regenerating mouse ear. Semin Cell Dev Biol. 1999;10(4):415–419. [PubMed: 10497098]
3. Fitzgerald J, Rich C, Burkhardt D, Allen J, Herzka AS, Little CB. Evidence for articular cartilage regeneration in MRL/MpJ mice. Osteoarthr Cartil. 2008;16(11):1319–1326. [PubMed: 18455447]
4. Ueno M, Lyons BL, Burzenski LM, et al. Accelerated wound healing of alkali-burned corneas in MRL mice is associated with a reduced inflammatory signature. Investig Ophthalmol Vis Sci. 2005;46(11):4097–4106. [PubMed: 16249486]
5. Colwell AS, Krummel TM, Kong W, Longaker MT, Lorenz HP. Skin wounds in the MRL/MPJ mouse heal with scar. Wound Repair Regen. 2006;14(1):81–90. [PubMed: 16476076]
6. Paredes J, Shiovitz DA, Andarawis-Puri N. Uncorrelated healing response of tendon and ear injuries in MRL highlight a role for the local tendon environment in driving scarless healing. Connect Tissue Res. 2018;59(5):472–482. [PubMed: 29929396]
7. Sereysky JB, Flatow EL, Andarawis-Puri N. Musculoskeletal regeneration and its implications for the treatment of tendinopathy. Int J Exp Pathol. 2013;94(4):293–303. [PubMed: 23772908]
8. Lalley AL, Dyment NA, Kazemi N, et al. Improved biomechanical and biological outcomes in the MRL/MpJ murine strain following a full-length patellar tendon injury. J Orthop Res. 2015;33(11):1693–1703. [PubMed: 25982892]
9. Gilpin A, Yang Y. Decellularization strategies for regenerative medicine: from processing techniques to applications. Biomed Res Int. 2017;2017:9831534. [PubMed: 28540307]
10. Xue A, Niu G, Chen Y, et al. Recellularization of well-preserved decellularized kidney scaffold using adipose tissue-derived stem cells. J Biomed Mater Res A. 2018;106(3):805–814. [PubMed: 29067774]
11. DeQuach JA, Lin JE, Cam C, et al. Injectable skeletal muscle matrix hydrogel promotes neovascularization and muscle cell infiltration in a hindlimb ischemia model. Eur Cell Mater. 2012;23:400–412; discussion 412. [PubMed: 22665162]
12. Singelyn JM, DeQuach JA, Seif-Naraghi SB, Littlefield RB, Schup-Magoffin PJ, Christman KL. Naturally derived myocardial matrix as an injectable scaffold for cardiac tissue engineering. Biomaterials. 2009;30(29):5409–5416. [PubMed: 19608268]
13. Clark LD, Clark RK, Heber-Katz E. A new murine model for mammalian wound repair and regeneration. Clin Immunol Immunopathol. 1998;88(1):35–45. [PubMed: 9683548]
14. Gawriluk TR, Simkin J, Thompson KL, et al. Comparative analysis of ear-hole closure identifies epimorphic regeneration as a discrete trait in mammals. Nat Commun. 2016;7:11164. [PubMed: 27109826]
15. Franchi M, Trire A, Quaranta M, Orsini E, Ottani V. Collagen structure of tendon relates to function. ScientificWorldJournal. 2007;7:404–420. [PubMed: 17450305]
16. Snedeker JG, Foolen J. Tendon injury and repair - A perspective on the basic mechanisms of tendon disease and future clinical therapy. Acta Biomater. 2017;63:18–36. [PubMed: 28867648]
17. Eriksen HA, Pajala A, Leppilahti J, Risteli J. Increased content of type III collagen at the rupture site of human Achilles tendon. J Orthop Res. 2002;20(6):1352–1357. [PubMed: 12472252]
18. Dunkman AA, Buckley MR, Mienaltowski MJ, et al. The tendon injury response is influenced by decorin and biglycan. Ann Biomed Eng. 2014;42(3):619–630. [PubMed: 24072490]
19. Svensson L, Aszodi A, Reinholt FP, Fassler R, Heinegard D, Oldberg A. Fibromodulin-null mice have abnormal collagen fibrils, tissue organization, and altered lumican deposition in tendon. J Biol Chem. 1999;274(14):9636–9647. [PubMed: 10092650]

20. Screen HRC, Berk DE, Kadler KE, Ramirez F, Young MF. Tendon functional extracellular matrix. J Orthop Res. 2015;33(6):793–799. [PubMed: 25640030]
21. Vorotnikova E, McIntosh D, Dewilde A, et al. Extracellular matrix-derived products modulate endothelial and progenitor cell migration and proliferation in vitro and stimulate regenerative healing in vivo. Matrix Biol. 2010;29(8):690–700. [PubMed: 20797438]
22. Gillies AR, Smith LR, Lieber RL, Varghese S. Method for decellularizing skeletal muscle without detergents or proteolytic enzymes. Tissue Eng Part C Methods. 2011;17(4):383–389. [PubMed: 20973753]
23. Beason DP, Kuntz AF, Hsu JE, Miller KS, Soslowsky LJ. Development and evaluation of multiple tendon injury models in the mouse. J Biomech. 2012;45(8):1550–1553. [PubMed: 22405494]
24. Kannus P Structure of the tendon connective tissue. Scand J Med Sci Sports. 2000;10(6):312–320. [PubMed: 11085557]
25. Svensson RB, Mulder H, Kovanen V, Magnusson SP. Fracture mechanics of collagen fibrils: influence of natural cross-links. Biophys J. 2013;104(11):2476–2484. [PubMed: 23746520]
26. Li Y, Fessel G, Georgiadis M, Snedeker JG. Advanced glycation end-products diminish tendon collagen fiber sliding. Matrix Biol. 2013;32(3–4):169–177. [PubMed: 23348249]
27. Marturano JE, Xylas JF, Sridharan GV, Georgakoudi I, Kuo CK. Lysyl oxidase-mediated collagen crosslinks may be assessed as markers of functional properties of tendon tissue formation. Acta Biomater. 2014;10(3):1370–1379. [PubMed: 24316363]
28. Christiansen DL, Huang EK, Silver FH. Assembly of type I collagen: fusion of fibril subunits and the influence of fibril diameter on mechanical properties. Matrix Biol. 2000;19(5):409–420. [PubMed: 10980417]
29. Erisken C, Zhang X, Moffat KL, Levine WN, Lu HH. Scaffold fiber diameter regulates human tendon fibroblast growth and differentiation. Tissue Eng Part A. 2013;19(3–4):519–528. [PubMed: 23150905]
30. Hildebrand A, Romaris M, Rasmussen LM, et al. Interaction of the small interstitial proteoglycans biglycan, decorin and fibromodulin with transforming growth factor beta. Biochem J. 1994; 302(Pt 2):527–534. [PubMed: 8093006]
31. Abdel-Wahab N, Wicks SJ, Mason RM, Chantry A. Decorin suppresses transforming growth factor-beta-induced expression of plasminogen activator inhibitor-1 in human mesangial cells through a mechanism that involves Ca2+-dependent phosphorylation of Smad2 at serine-240. Biochem J. 2002;362(Pt 3):643–649. [PubMed: 11879191]
32. Wang L, Foster BL, Kram V, et al. Fibromodulin and biglycan modulate periodontium through TGFbeta/BMP signaling. J Dent Res. 2014;93(8):780–787. [PubMed: 24966230]
33. Bi Y, Ehirchiou D, Kilts TM, et al. Identification of tendon stem/ progenitor cells and the role of the extracellular matrix in their niche. Nat Med. 2007;13(10):1219–1227. [PubMed: 17828274]
34. Zheng Z, Zhang X, Dang C, et al. Fibromodulin is essential for fetal-type scarless cutaneous wound healing. Am J Pathol. 2016;186(11):2824–2832. [PubMed: 27665369]
35. Honardoust D, Varkey M, Marcoux Y, Shankowsky HA, Tredget EE. Reduced decorin, fibromodulin, and transforming growth factor-beta3 in deep dermis leads to hypertrophic scarring. J Burn Care Res. 2012;33(2):218–227. [PubMed: 22079916]
36. Zheng Z, James AW, Li C, et al. Fibromodulin reduces scar formation in adult cutaneous wounds by eliciting a fetal-like phenotype. Signal Transduct Target Ther. 2017;2(1).
37. Porzionato A, Stocco E, Barbon S, Grandi F, Macchi V, De Caro R. Tissue-engineered grafts from human decellularized extracellular matrices: a systematic review and future perspectives. Int J Mol Sci. 2018;19(12):4117.
38. Taylor DA, Sampaio LC, Ferdous Z, Gobin AS, Taite LJ. Decellularized matrices in regenerative medicine. Acta Biomater. 2018;74:74–89. [PubMed: 29702289]
39. Hoshiba T, Lu H, Kawazoe N, Chen G. Decellularized matrices for tissue engineering. Expert Opin Biol Ther. 2010;10(12):1717–1728. [PubMed: 21058932]
40. Hussey GS, Dziki JL, Badylak SF. Extracellular matrix-based materials for regenerative medicine. Nat Rev Mater. 2018;3(7):159–173.

41. Chen WCW, Wang Z, Missinato MA, et al. Decellularized zebrafish cardiac extracellular matrix induces mammalian heart regeneration. Science Advances. 2016;2(11):e1600844. [PubMed: 28138518]
42. Rao N, Agmon G, Tierney MT, et al. Engineering an injectable muscle-specific microenvironment for improved cell delivery using a nanofibrous extracellular matrix hydrogel. ACS Nano. 2017;11(4):3851–3859. [PubMed: 28323411]
43. Zhang L, Zhang F, Weng Z, et al. Effect of an inductive hydrogel composed of urinary bladder matrix upon functional recovery following traumatic brain injury. Tissue Eng Part A. 2013;19(17–18):1909–1918. [PubMed: 23596981]
44. Poon CJ, Pereira E. Cotta MV, Sinha S, et al. Preparation of an adipogenic hydrogel from subcutaneous adipose tissue. Acta Biomater. 2013;9(3):5609–5620. [PubMed: 23142702]
45. Subramanian A, Kanzaki LF, Galloway JL, Schilling TF. Mechanical force regulates tendon extracellular matrix organization and tenocyte morphogenesis through TGFbeta signaling. Elife. 2018;7:e38069. [PubMed: 30475205]
46. Banes AJ, Weinhold P, Yang X, et al. Gap junctions regulate responses of tendon cells ex vivo to mechanical loading. Clin Orthop Relat Res. 1999;367:S356–S370.
47. Richardson SH, Starborg T, Lu Y, Humphries SM, Meadows RS, Kadler KE. Tendon development requires regulation of cell condensation and cell shape via cadherin-11-mediated cell-cell junctions. Mol Cell Biol. 2007;27(17):6218–6228. [PubMed: 17562872]
48. Born A-K, Rottmar M, Lischer S, Pleskova M, Bruinink A, Maniura-Weber K. Correlating cell architecture with osteogenesis: first steps towards live single cell monitoring. Eur Cell Mater. 2009;18:49–60, 61–62; discussion 60.
49. Al-sadi O, Schulze-Tanzil G, Kohl B, Lohan A, Lemke M, John T. Tenocytes, pro-inflammatory cytokines and leukocytes: a relationship? Muscles Ligaments Tendons J. 2011;1(8):68–76. [PubMed: 23738251]
50. Disser NP, Sugg KB, Talarek JR, Sarver DC, Rourke BJ, Mendias CL. Insulin-like growth factor 1 signaling in tenocytes is required for adult tendon growth. FASEB J. 2019;33(11):12680–12695. [PubMed: 31536390]
51. Costa MA, Wu C, Pham BV, Chong AKS, Pham HM, Chang J. Tissue engineering of flexor tendons: optimization of tenocyte proliferation using growth factor supplementation. Tissue Eng. 2006;12(7):1937–1943. [PubMed: 16889523]
52. Moon DK, Abramowitch SD, Woo SL-Y. The development and validation of a charge-coupled device laser reflectance system to measure the complex cross-sectional shape and area of soft tissues. J Biomech. 2006;39(16):3071–3075. [PubMed: 16413929]
53. Pokhai GG, Oliver ML, Gordon KD. A new laser reflectance system capable of measuring changing cross-sectional area of soft tissues during tensile testing. J Biomech Eng. 2009;131(9):94504.
54. Blankenhorn EP, Troutman S, Clark LD, Zhang X-M, Chen P, Heber-Katz E. Sexually dimorphic genes regulate healing and regeneration in MRL mice. Mamm Genome. 2003;14(4):250–260. [PubMed: 12682777]
55. Heber-Katz E, Chen P, Dvm LC, Zhang X-M, Troutman S, Blankenhorn EP. Regeneration in MRL mice: further genetic loci controlling the ear hole closure trait using MRL and M.m. Castaneus mice. Wound Repair Regen. 2004;12(3):384–392. [PubMed: 15225218]

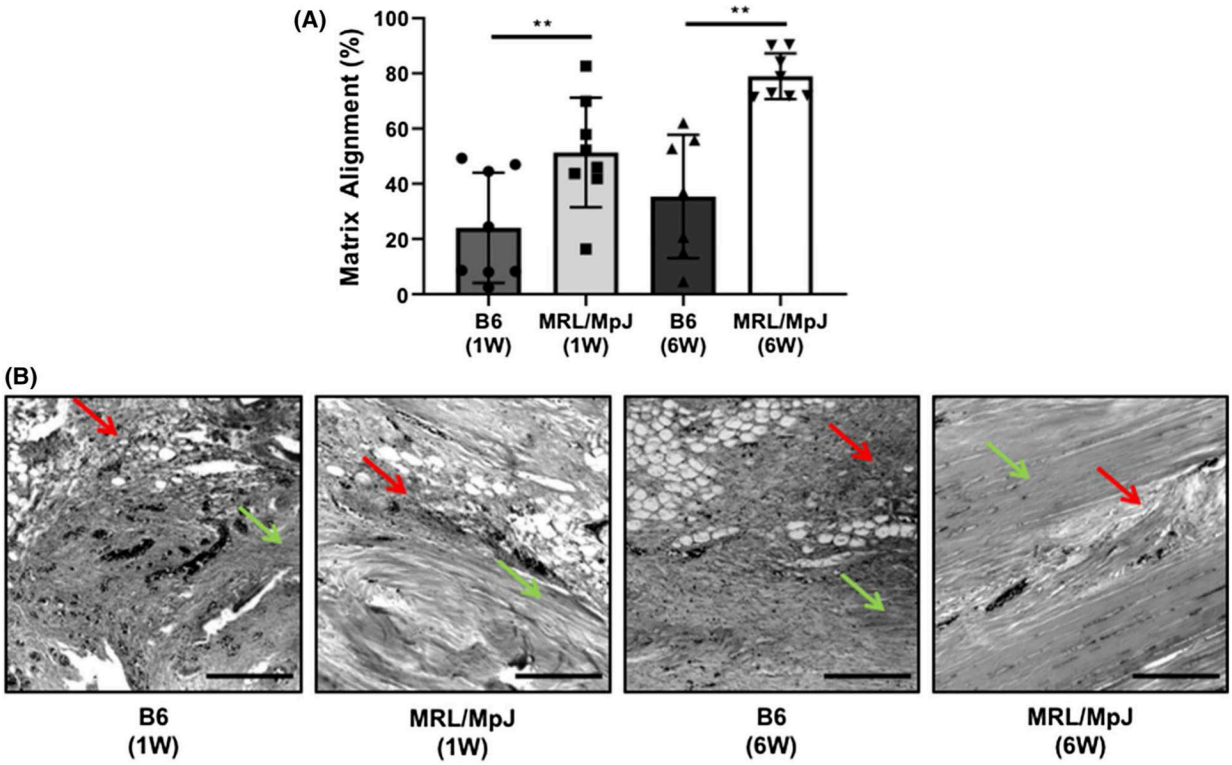

FIGURE 1.

(A) Analysis of structural matrix alignment in healing MRL/MpJ and C57BL/6 (B6) tendons. MRL/MpJ showed higher levels of matrix alignment compared to B6 at both 1 week (W) and 6W post in vivo healing. (B) Micrographs show representative histological sections of B6 (1W), MRL/MpJ (1W), B6 (6W), and MRL/MpJ (6W), respectively. Red arrows mark representative regions of matrix disorganization, while green arrows mark representative regions of alignment. Scale bars represent 200 μm. $^{**}P \leq .01$

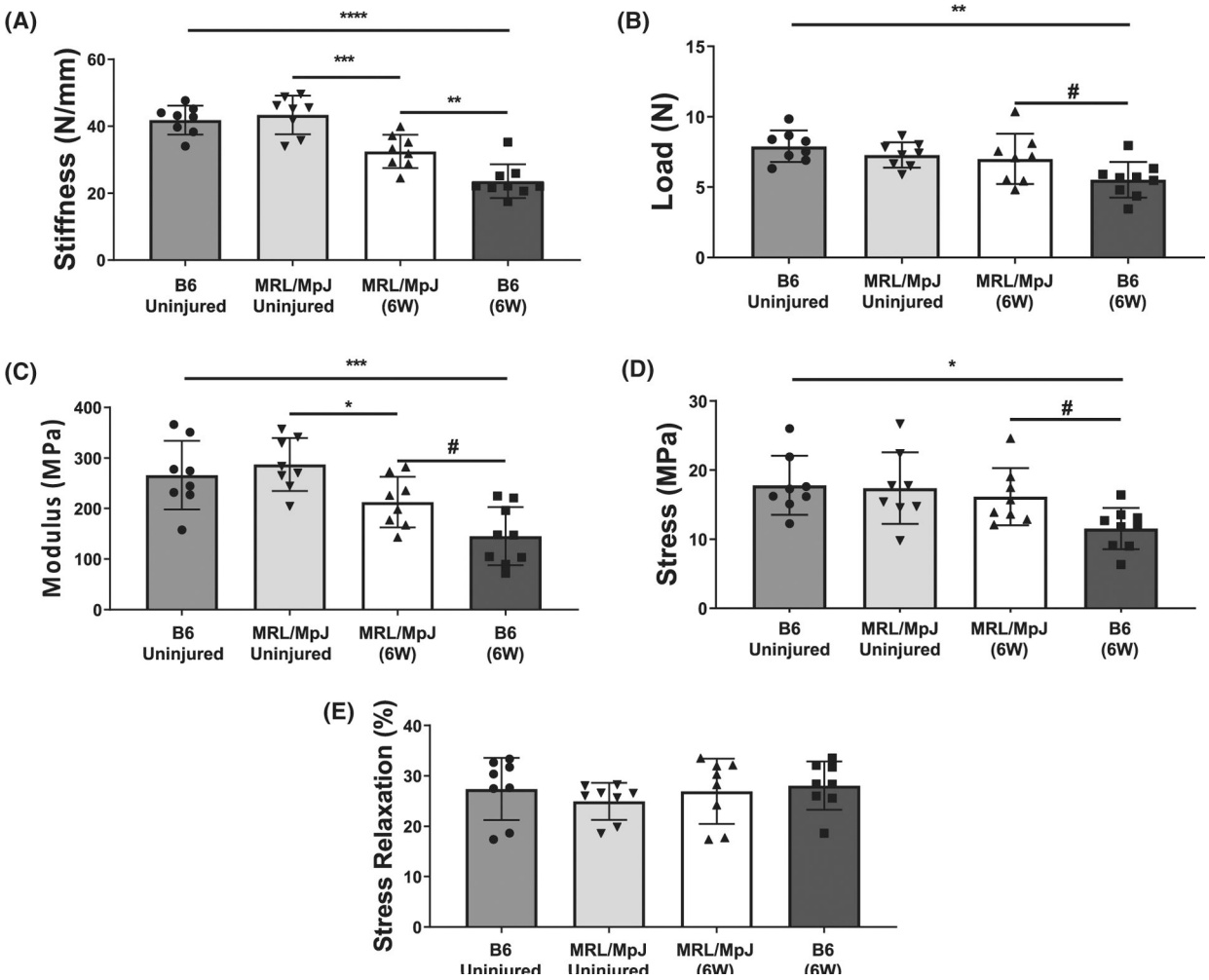

FIGURE 2.

Mechanical assessment of MRL/MpJ and B6 patellar tendons 6 weeks (W) following a midsubstance punch injury. Healing B6 tendons exhibited decreased stiffness (A) and ultimate load (B), while healing MRL/MpJ tendons exhibited decreased stiffness (A) compared to uninjured controls after 6W. However, MRL/MpJ tendons showed higher stiffness (A) and ultimate load (B) compared to B6 after healing for 6W in vivo. Material properties showed improvements in (C) Young's modulus and (D) ultimate stress in injured MRL/MpJ tendons compared to B6. Injured MRL/MpJ and B6 tendons exhibited decreases in Young's Modulus, however, only B6 injured tendons showed differences in ultimate stress compared to uninjured controls at 6W. E, Stress relaxation (%) was similar between all groups evaluated. $\#P < .1$, $*P < .05$, $**P \leq .01$, $***P \leq .001$, $****P \leq .0001$

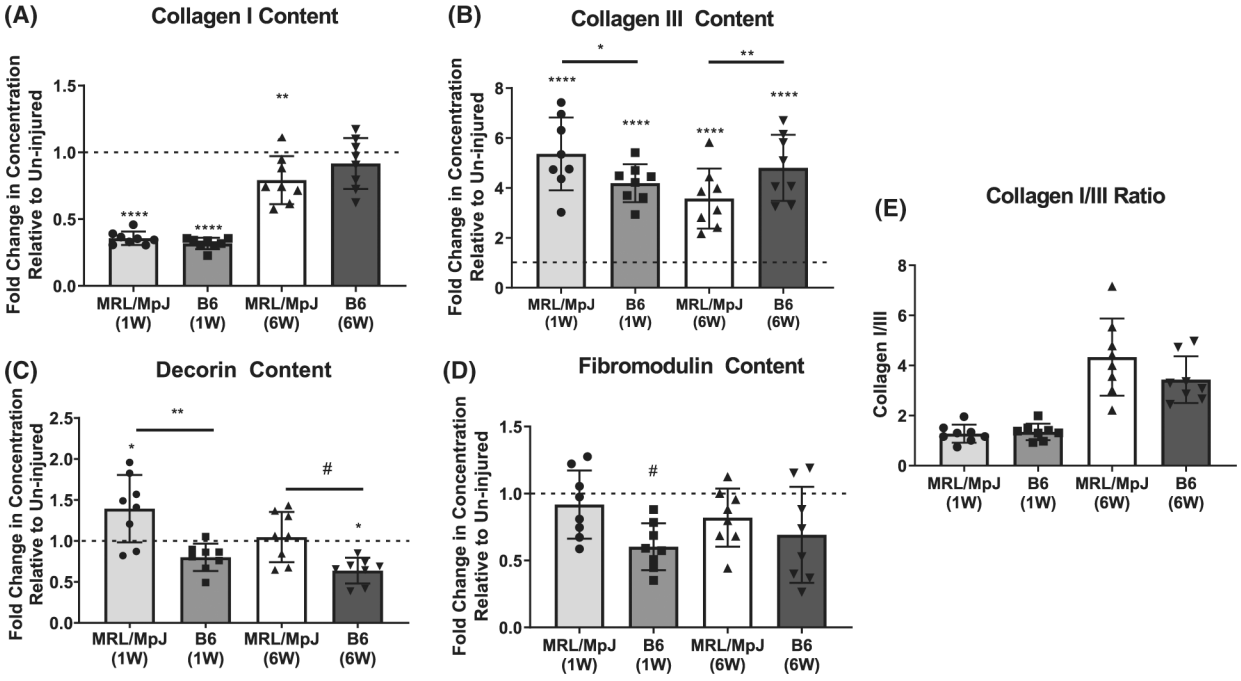

FIGURE 3.

Assessment of key structural matrix proteins in healing MRL/MpJ and B6 tendons. (A) Collagen I was decreased in healing MRL/MpJ and B6 tendons compared to controls at 1 week (W) but was recovered to uninjured levels in B6 by 6W. (B) While elevated in all healing groups at 1W and 6W, collagen III was more elevated in healing MRL/MpJ than healing B6 tendons at 1W, but was less elevated in healing MRL/MpJ than healing B6 tendons at 6W. (C) Decorin was increased at 1W in healing MRL/MpJ tendons compared to controls and healing B6 tendons. At 6W decorin returned to uninjured levels in the MRL/MpJ while it was decreased in healing B6 tendons compared to uninjured controls. (D) Fibromodulin was decreased only in healing B6 tendons by 1W and returned to uninjured levels by 6W. (A-D) Dotted line represents protein concentration in uninjured controls respective to strain, and symbol above group denotes difference compared to uninjured control. (E) No differences were found in the collagen I/III ratio at 1 or 6W across strains. Protein concentrations were normalized to respective total protein content for all groups. *#P* ≤ .1, **P* ≤ .05, ***P* ≤ .01, *****P* ≤ .0001

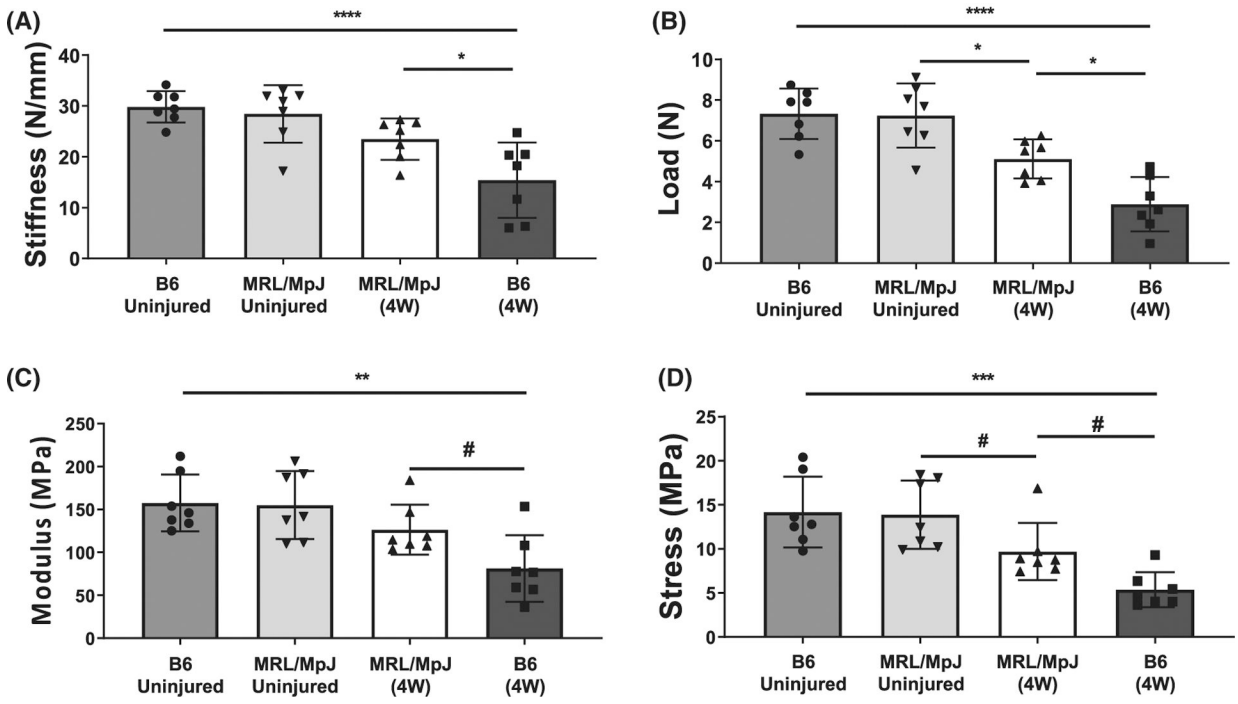

FIGURE 4.

Mechanical assessment of MRL/MpJ and B6 patellar tendons following 4 weeks in organ culture. No differences were found in stiffness (A), or ultimate load (B) between uninjured MRL/MpJ and B6 patellar tendons due to the organ culture environment. While still lower than controls, healing MRL/MpJ tendons showed improved stiffness and ultimate load compared to B6 at 4W post-culture. Injured MRL/ MpJ tendons showed higher Young's Modulus (C), and ultimate stress (D) compared to injured B6 after 4 weeks in culture. Injured MRL/MpJ tendons showed a decreased ultimate stress, while decreases in both Young's Modulus and ultimate stress were identified in injured B6 tendons compared to respective uninjured controls (C,D). $\#P \leq .1$, $^{**}P \leq .01$, $^{****}P \leq .0001$

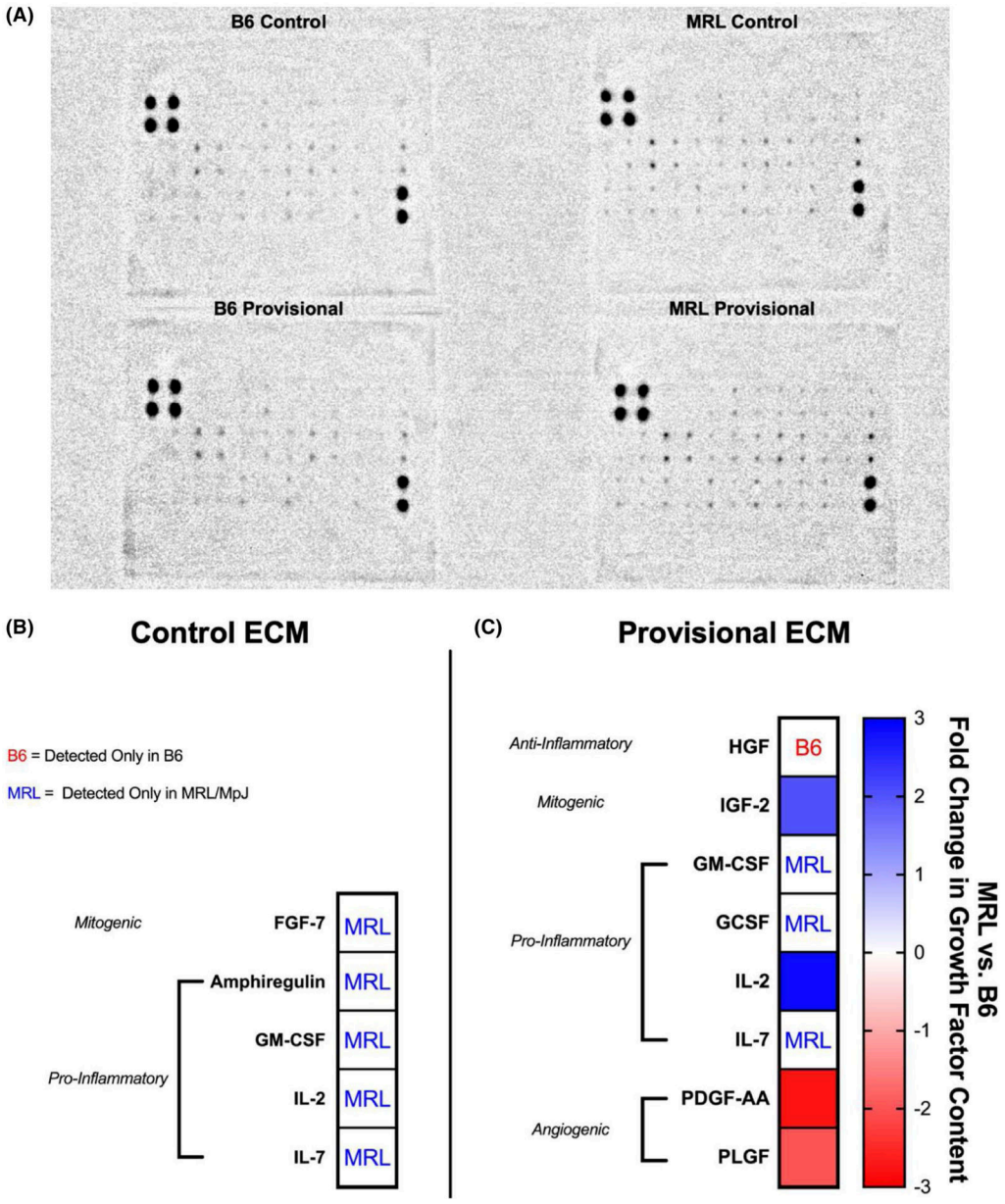

FIGURE 5.

Semiquantitative evaluation of growth factor content (MRL/MpJ relative to B6) in decellularized uninjured control and 1-week provisional-ECM digests. Growth factor content is presented as fold change expression. (*A*) Representative image of the RayBiotech C-Series Mouse Growth Factor Antibody Array used to analyze decellularized B6 and MRL/MpJ ECM digests. (*B)* MRL/MpJ control ECM contained pro-inflammatory cytokines and mitogenic growth factors that were not detected in B6 control ECM (*C)* A greater number of differentially regulated growth factors was found between B6 and MRL/MpJ provisional-ECM. Pro-inflammatory cytokines and mitogenic growth factors were elevated in MRL/MpJ provisional-ECM compared to B6 provisional-ECM. Anti-inflammatory cytokines and angiogenic growth factors were reduced in MRL/MpJ provisional-ECM

compared to B6 provisional-ECM. Fold changes in growth factor content are visualized by the heat map where warm colors denote increased content in B6 ECM, whereas cool colors denote increased content in MRL/MpJ ECM. “B6” denotes a growth factor detected only in B6 ECM, “MRL” denotes a growth factor detected only in MRL/MpJ ECM

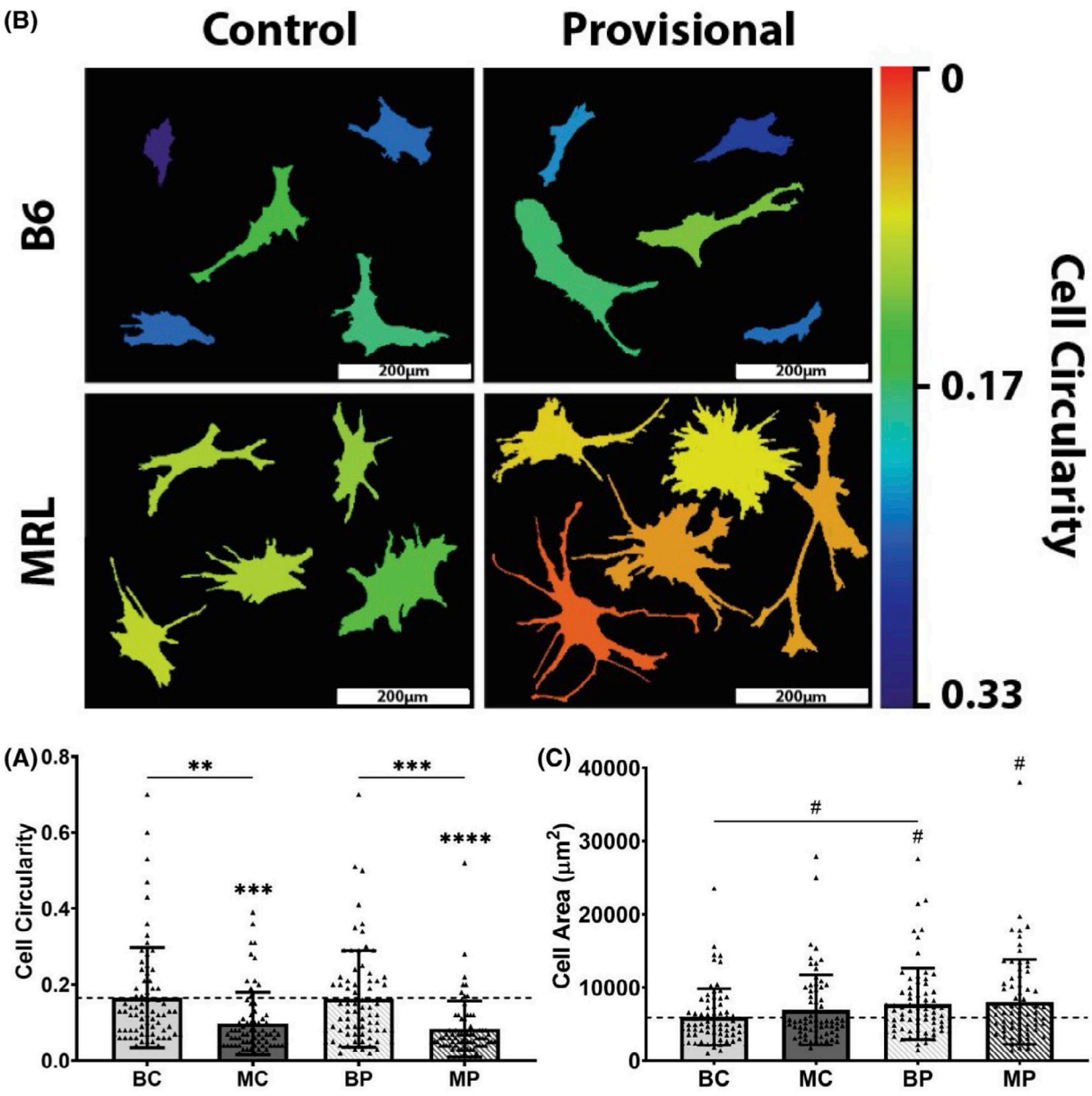

FIGURE 6.

Single-cell analysis of actin cytoskeletal organization of B6 patellar tendon cells cultured on decellularized control and 1-week provisional-ECM coatings. (*A*) Thresholded outlines of five representative cells. MRL/MpJ 1-week provisional-ECM coatings increased cell spreading and promoted the formation of visually apparent cellular protrusions, whereas B6 ECM coatings maintained comparable cell morphology to collagen type I control. Quantified measurements of cell circularity are visualized by the heat map where warm colors denote decreased cell circularity, whereas cool colors denote increased cell circularity. Scale bars: 200 μm. (*B*) Quantification of cell circularity. (*C*) Quantification of cell area. Dotted line represents mean of collagen type I control. #$P < .1$, *$P < .05$, **$P < .01$, ***$P < .001$, ****$P < .0001$. Symbol above group denotes difference compared to collagen I control

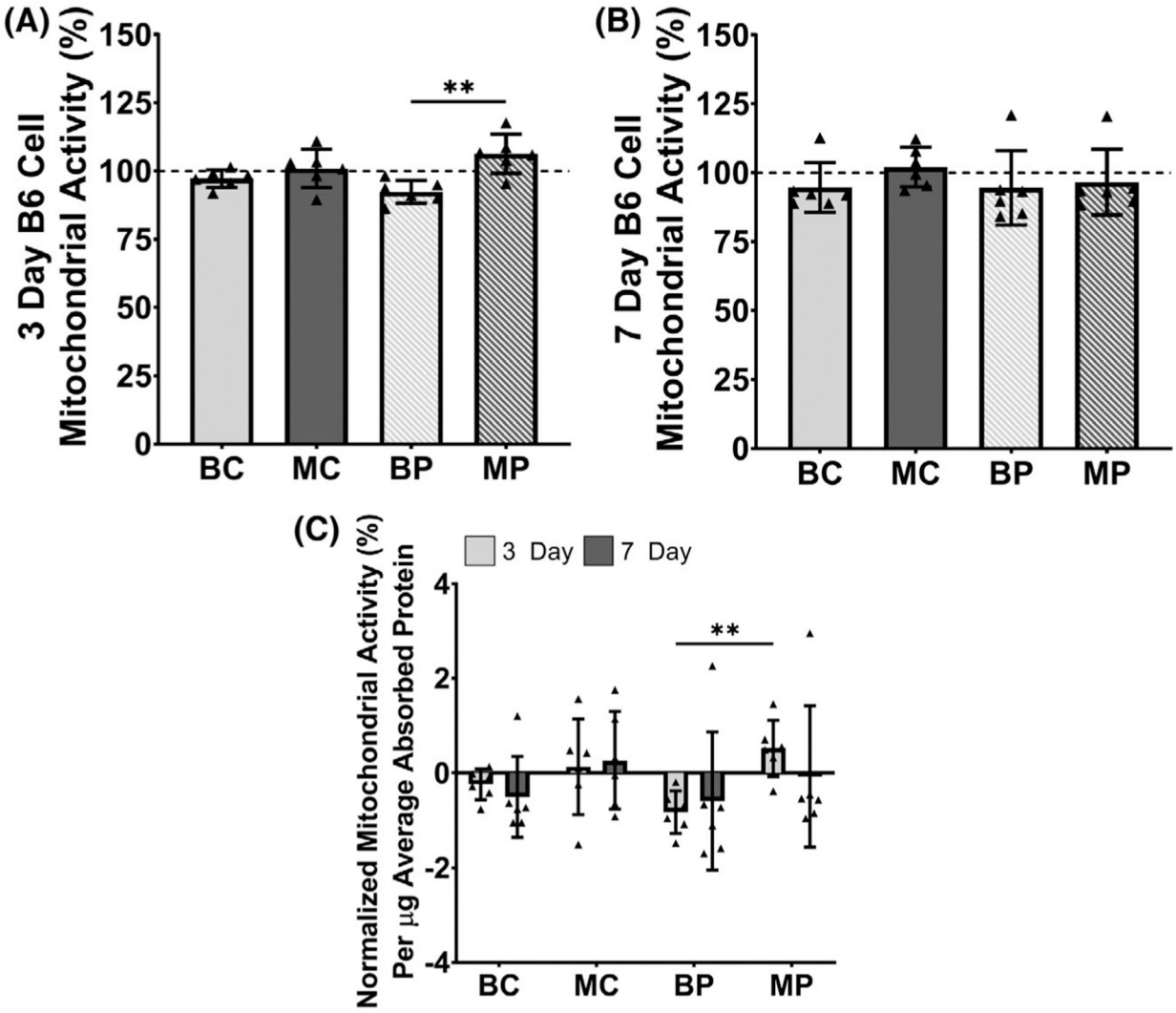

FIGURE 7.

Cell proliferation of B6 patellar tendon cells cultured on decellularized control and 1-week provisional-ECM coatings via mitochondrial activity measured using an MTS assay. Mitochondrial activity was normalized to that of a non-coated control (ie, cells cultured in media without ECM). (*A*) After 3 days of culture, mitochondrial activity was significantly enhanced on MRL/MpJ 1-week provisional-ECM coatings. (B) After 7 days of culture, no significant differences in mitochondrial activity were found for all selected statistical comparisons. (*C*) Relative cell proliferation was normalized on a per microgram basis to the initial total protein adsorbed by each ECM coating. After 3 days of culture, MRL/MpJ 1-week provisional-ECM coatings significantly enhanced the mitochondrial activity of B6 cells compared to B6 1-week provisional-ECM coatings. Dotted lines indicate mean of the non-coated control. $^{**}P \leq .01$

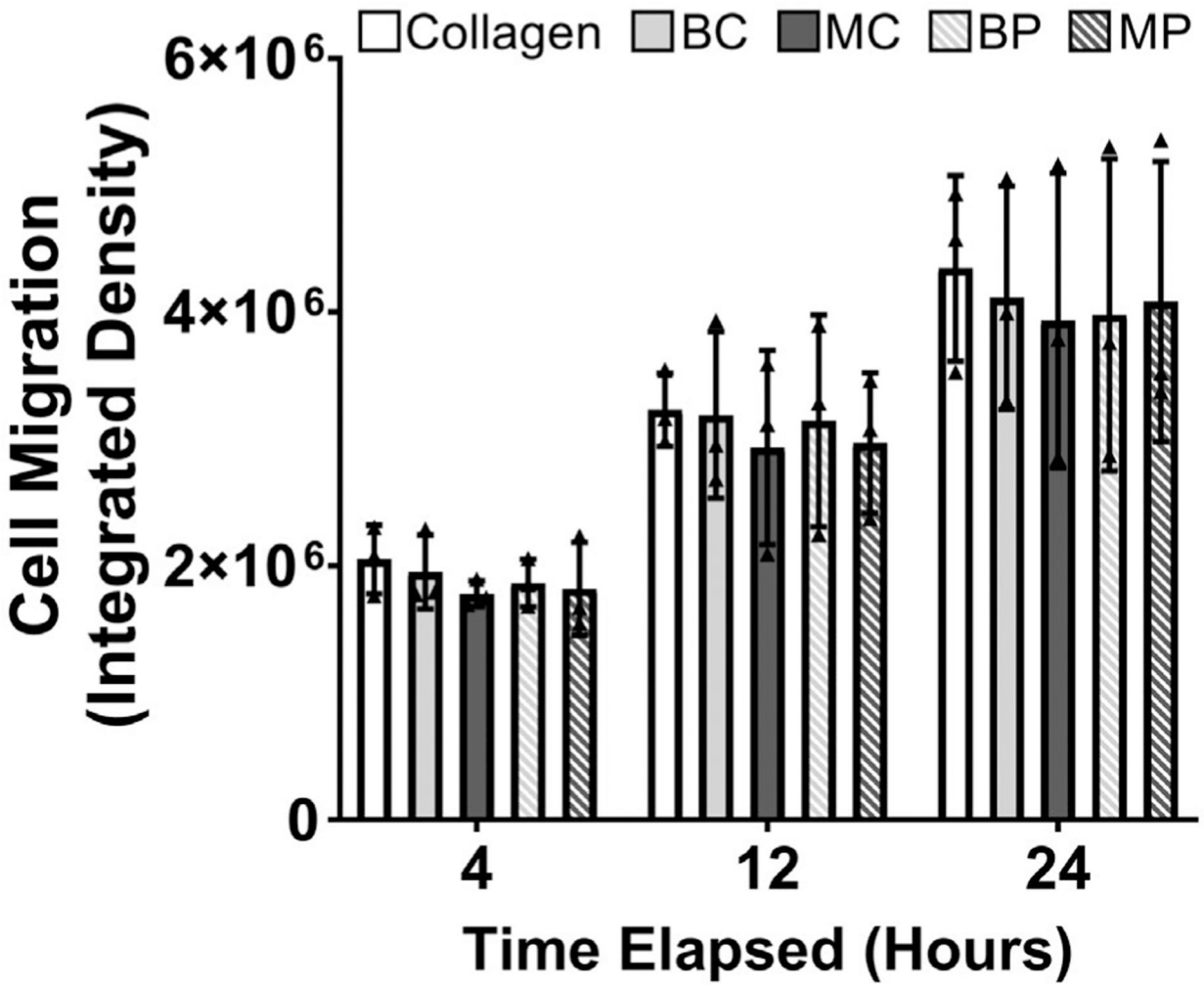

FIGURE 8.

Cell migration of B6 patellar tendon cells cultured on collagen control and decellularized B6 and MRL/MpJ ECM coatings via integrated density of fluorescence micrographs. No differences in cell migration were found for cells cultured between different ECM coating groups at any of the timepoints measured